Magnetic spectral signatures in the terrestrial plasma depletion layer: Hybrid simulations

Q. M. Lu,[1] F. Guo,[1] and S. Wang[1]

Received 4 September 2005; revised 30 November 2005; accepted 12 January 2006; published 12 April 2006.

[1] The electromagnetic ion cyclotron waves in the terrestrial plasma depletion layer (PDL) are characterized by three different spectral categories. They are LOW, where the ion cyclotron waves have a continuous spectrum with main power below $0.5\Omega_p$ (Ω_p is the proton gyrofrequency); CON, where the main power in the continuous spectrum of the waves can extend from $\sim$0.1 up to $1.0\Omega_p$; and BIF, where a diminution around $0.5\Omega_p$ occurs between two activity peaks in the spectrum. These magnetic fluctuations in the PDL are considered to be the combined effects of two types of ion cyclotron waves: proton cyclotron waves and helium cyclotron waves, which are excited by the H^+ and He^{2+} temperature anisotropies, respectively. In this paper, with one-dimensional (1-D) hybrid simulations we investigate the nonlinear evolution of the ion cyclotron waves excited by the H^+ and He^{2+} temperature anisotropies. The proton cyclotron waves with the dominant frequency (the amplitude at that frequency is largest in the spectrum) larger than $0.5\Omega_p$ are first excited, and then the helium cyclotron waves with the dominant frequency smaller than $0.5\Omega_p$ are excited. The frequencies of the proton cyclotron waves decrease in their corresponding nonlinear stage. For $\beta_{\|p} = 0.1$ (where $\beta_{\|p}$ is the parallel proton plasma beta), the dominant frequency of the proton cyclotron waves remains around $0.62\Omega_p$ because of the He^{2+} absorption around the helium gyrofrequency. Therefore, after the helium cyclotron waves with the dominant frequency around $0.25\Omega_p$ are excited, there exist two activity peaks in the spectrum. At the quasi-equilibrium stage, the amplitude of the proton cyclotron waves is very small because of the He^{2+} absorption, and a continuous spectrum with main power below $0.5\Omega_p$ is formed. When $\beta_{\|p} = 0.3$, the effect of the He^{2+} absorption is very small and can be neglected. The frequencies of the proton cyclotron waves decrease in their nonlinear evolution. After the helium cyclotron waves are excited, their frequency band merges with that of the proton cyclotron waves and forms a continuous spectrum with main power extending above $0.5\Omega_p$. At the quasi-equilibrium stage, with the decrease of the frequencies of the ion cyclotron waves a continuous spectrum with main power below $0.5\Omega_p$ is formed. The relations between the three different spectral categories observed in the PDL and the spectra during the evolution of the ion cyclotron waves are also discussed. The results on the spectrum evolution of the ion cyclotron waves excited by the H^+ and He^{2+} temperature anisotropies may help to explain the magnetic spectral signatures observed in the PDL.

Citation: Lu, Q. M., F. Guo, and S. Wang (2006), Magnetic spectral signatures in the terrestrial plasma depletion layer: Hybrid simulations, *J. Geophys. Res.*, *111*, A04207, doi:10.1029/2005JA011405.

1. Introduction

[2] Adjacent to the sunward side of the low-shear dayside magnetopause, there exists a region characterized by reduced plasma density and increased magnetic field strength. This region is called plasma depletion layer (PDL), which is formed by the stretching of magnetic field lines and consequent pileup of the magnetic field as the magnetosheath plasma approaches the magnetopause. This generation mechanism for the PDL was proposed by numerous authors [e.g., *Midgley and Davis*, 1963; *Zwan and Wolf*, 1976; *Wu*, 1992], and it was also confirmed by spacecraft observations [*Paschmann et al.*, 1978; *Crooker et al.*, 1979; *Phan et al.*, 1994].

[3] Spacecraft observations show that there are a wide variety of magnetic fluctuations in the PDL. The magnetic fluctuations are predominantly transverse to the background field and their frequencies can be up to the proton gyrofrequency. Detailed analysis shows that the fluctuations are mainly electromagnetic ion cyclotron waves excited by the H^+ and He^{2+} temperature anisotropies [*Anderson et al.*, 1991, 1994; *Anderson and Fuselier*, 1993; *Fuselier et al.*,

[1]CAS Key Laboratory of Basic Plasma Physics, School of Earth and Space Sciences, University of Science and Technology of China, Hefei, China.

0148-0227/06/2005JA011405$09.00

1994]. *Anderson and Fuselier* [1993] and *Anderson et al.* [1994] showed that the higher-frequency band is left-hand polarized while the lower-frequency band is linearly polarized, and *Denton et al.* [1993] attributed the linear polarization of the lower-frequency band to its wave vector oblique to the background magnetic field. Analytical theory and hybrid simulations have predicted that the ion temperature anisotropies can excite both ion cyclotron waves and compressive mirror waves [*Winske and Quest*, 1988; *Gary*, 1992; *McKean et al.*, 1992; *Anderson and Fuselier*, 1993; *Anderson et al.*, 1994]. However, in the PDL the proton plasma beta is usually $\beta_p < 1$, in such situation the magnetic fluctuations excited by the temperature anisotropies are mainly ion cyclotron waves while the compressive mirror-mode waves can be neglected [*Anderson et al.*, 1991; *Anderson*, 1995; *Gary et al.*, 1994a, 1994b, 1997; *Denton et al.*, 1993, 1994a, 1995; *Farrugia et al.*, 2004]. One of possible mechanisms for such temperature anisotropies is due to the heating of the quasi-perpendicular shock [*Leory et al.*, 1982; *Sckopke et al.*, 1990; *McKean et al.*, 1995; *Fuselier and Schmidt*, 1997; *Lu and Wang*, 2005], and observations have indicated that the PDL preferentially forms when the upstream shock is quasi-perpendicular [*Anderson and Fuselier*, 1993]. In addition to this mechanism, the temperature anisotropies can also be driven by the perpendicular compression of flux tubes at the magnetopause and flux tube stretching along the magnetic field around the magnetopause [*Denton et al.*, 1994b, 1995; *Pudovkin et al.*, 1999; *Erkaev et al.*, 1999, 2000; *Denton and Lyon*, 2000; *Samsonov et al.*, 2001; *Hellinger and Travnicek*, 2005]. Spacecraft observations also demonstrate an anticorrelation between A_p($A_p = \mathrm{T}_{\perp p}/\mathrm{T}_{\parallel p} - 1$, where the subscript p denotes H^+, the subscripts $\parallel$ and $\perp$ denote the directions parallel and perpendicular to the ambient magnetic field, respectively) and the parallel proton plasma beta $\beta_{\parallel p}$ in the PDL [*Anderson and Fuselier*, 1993; *Fuselier et al.*, 1994; *Anderson et al.*, 1994]. Analytic theory and hybrid simulations [*Gary et al.*, 1994a, 1994b, 1997] have shown that this correlation is a special case of the more general result of an upper bound on the proton anisotropy imposed by the electromagnetic proton cyclotron anisotropy instability.

[4] Besides these, AMPTE/CCE [*Anderson and Fuselier*, 1993; *Anderson et al.*, 1994] and Wind [*Farrugia et al.*, 2004] spacecraft observed that ion cyclotron waves inside the PDL have three different spectral categories, called LOW, CON and BIF respectively. *Anderson et al.* [1994] defined these categories as follows: (1) LOW, a continuous spectrum of the ion cyclotron waves with main power below $0.5\Omega_p$, where Ω_p is the proton gyrofrequency; (2) CON, a continuous spectrum with mainly power extending from $\sim$0.1 up to $1.0\Omega_p$; and (3) BIF, a spectrum characterized by two activity peaks, one above and one below $0.5\Omega_p$. With the linear Vlasov theory, *Denton et al.* [1993, 1994a] found that for the low $\beta_{\parallel p}$ there exist two frequency bands in the spectrum of the excited ion cyclotron waves, and it can explain the BIF category observed in the PDL. The higher-frequency band is driven by the H^+ temperature anisotropy, while the lower-frequency band is driven by the He^{2+} temperature anisotropy. With the increase of the $\beta_{\parallel p}$, the two unstable frequency bands merge and form a continuous frequency spectrum, and it can explain the CON category observed in the PDL. It was also found with the linear Vlasov theory that a relative speed between the H^+ and He^{2+} can eliminate the gap between the two frequency bands in the BIF category and forms a continuous spectrum [*Gratton and Farrugia*, 1996; *Gnavi et al.*, 2000]. The above results are based on the linear Vlasov theory that can only study the linear stage of the ion cyclotron waves. The nonlinear evolution of the ion cyclotron waves excited by the H^+ and He^{2+} temperature anisotropies has also been studied with hybrid simulations [*Denton et al.*, 1993; *Gary et al.*, 1993a, 1993b; *Gary and Winske*, 1993]. In this paper, in order to explain the generation mechanisms of the three spectral categories in the PDL, we perform one-dimensional (1-D) hybrid simulations to investigate the spectrum evolution of the ion cyclotron waves excited by the H^+ and He^{2+} temperature anisotropies.

Table 1. Simulation Parameters for Runs 1–7

Run	$\beta_{\parallel p}$	$T_{\perp p}/T_{\parallel p}$	$T_{\perp\alpha}/T_{\parallel\alpha}$	η
1	0.1	3.8	4.56	0.04
2	0.1	3.8	1.0	0.04
3	0.1	1.0	4.56	0.04
4	0.1	3.8	···	0
5	0.3	3.8	4.56	0.04
6	0.3	3.8	1.0	0.04
7	0.3	1.0	4.56	0.04

[5] The paper is organized as follows: In section 2, the 1-D hybrid simulation results are presented. The discussion and conclusions are given in section 3, and their implications on observations are also presented in this section.

2. Simulation Model

[6] In the hybrid simulations the ions are treated kinetically while the electrons are considered as massless fluid [*Winske*, 1985; *Lu and Wang*, 2005]. The particles are advanced according to the well-known Boris algorithm while the electromagnetic fields are calculated with an implicit algorithm. The plasma consists of two ion components (H^+ and He^{2+}) and the electron component. Initially, both H^+ and He^{2+} satisfy bi-Maxwellian velocity distribution which bears zero average flow speed, and they have the same thermal velocity in the direction parallel to the ambient magnetic field.

[7] Periodic boundary conditions for the particles and fields are used in the simulations. The background magnetic field is assumed to be $\mathbf{B}_0 = B_0\hat{\mathbf{x}}$. In the simulations, units of space and time are c/ω_{pp} (where c/ω_{pp} is the proton inertial length, c and ω_{pp} are the light speed and proton plasma frequency, respectively) and Ω_p^{-1} (where $\Omega_p = eB_0/m_p$ is the proton gyro frequency). The number of the grid cells is $n_x = 256$, and the grid size is $\Delta x = 1.0c/\omega_{pp}$ with 500 particles per cell for each ion component. The time step is taken to be $\Omega_p t = 0.025$. The simulations are performed in the center-of-mass frame, where charge neutrality ($\sum_j e_j n_j = 0$ and the zero current condition ($\sum_j e_j n_j v_{0j} = 0$ are imposed at $t = 0$.

3. Simulation Results

[8] With 1-D hybrid simulations we investigate the spectrum evolution of the ion cyclotron waves excited by the H^+ and He^{2+} temperature anisotropies. The simulation parameters used in our simulations are listed in Table 1. In Table 1, $T_{\perp p}/T_{\parallel p}$ and $T_{\perp\alpha}/T_{\parallel\alpha}$ (where the subscript p denotes H^+, and

α denotes He^{2+}) are the H^+ and He^{2+} temperature anisotropies, respectively. $\eta = n_\alpha/(n_\alpha + n_p)$, where n_p is the number density for H^+, and n_α is the number density for He^{2+}.

[9] Figure 1 shows the time evolution of the H^+ and He^{2+} temperature anisotropies for run 1. With the excitation of the ion cyclotron waves, both the H^+ and He^{2+} temperature anisotropies decrease. Therefore the ion cyclotron waves include the proton cyclotron waves and helium cyclotron waves, which are excited by the H^+ and He^{2+} temperature anisotropy, respectively [*Gary et al.*, 1994b; *Lu and Wang*, 2005]. Because He^{2+} has smaller charge-to-mass ratio than H^+, the helium cyclotron waves are excited later than the proton cyclotron waves. The H^+ temperature anisotropy begins to decrease rapidly at $\Omega_p t \sim 20$, and reaches an almost constant at $\Omega_p t \sim 100$. The He^{2+} temperature anisotropy begins to decrease rapidly at $\Omega_p t \sim 100$, and a constant is reached at $\Omega_p t \sim 200$. At the quasi-equilibrium stage, the H^+ and He^{2+} temperature anisotropies are about 2.75 and 2.5, respectively.

[10] Figure 2 presents the spectrum evolution of the excited waves during four different time periods: A, from $\Omega_p t = 0$ to $\Omega_p t = 51.2$; B, from $\Omega_p t = 51.2$ to $\Omega_p t = 102.4$; C, from $\Omega_p t = 102.4$ to $\Omega_p t = 153.6$; and D, from $\Omega_p t = 204.8$ to $\Omega_p t = 256.0$ for run 1. The spectrum is calculated with the following procedure: we first calculate the spectrum by Fourier transforming the time series of the fluctuating magnetic field B_y at every grid point, and the spectrum shown in Figure 2 is the average value of all the grid points. During period A, the frequencies of the excited waves are around $0.62\Omega_p$, and the amplitude continues to increase during period B. From Figure 1, we can find that the waves excited during periods A and B are the proton cyclotron waves, and their frequencies can exceed the helium gyrofrequency $0.5\Omega_p$. During period C, with the excitation of the helium cyclotron waves, there appears another band in the spectrum with the frequencies around $\omega \sim 0.25\Omega_p$. Therefore there exist two frequency bands in the spectrum, and their peaks are around $0.25\Omega_p$ and $0.62\Omega_p$, respectively. The spectrum is similar to the BIF spectral category observed by

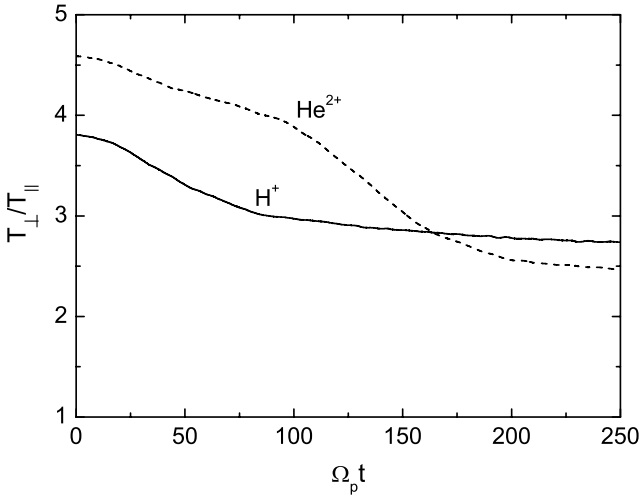

Figure 1. Time evolution of the H^+ and He^{2+} temperature anisotropies for run 1. The solid and dashed lines represent the H^+ and He^{2+} temperature anisotropies, respectively.

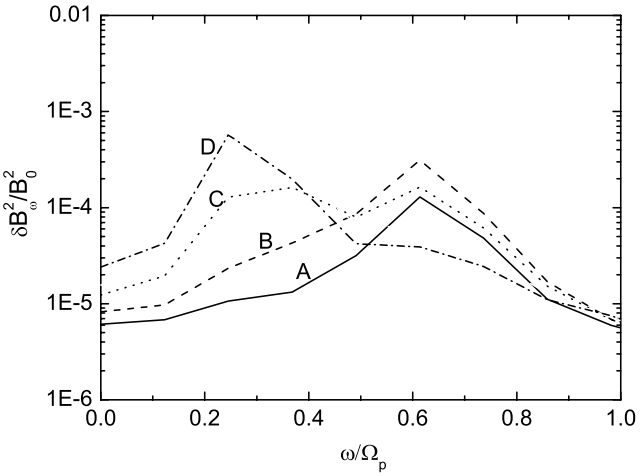

Figure 2. Frequency spectrum of the excited ion cyclotron waves during four different time periods for run 1. The solid, dashed, dotted and dash-dotted lines represent periods A, from $\Omega_p t = 0$ to $\Omega_p t = 51.2$; B, from $\Omega_p t = 51.2$ to $\Omega_p t = 102.4$; C, from $\Omega_p t = 102.4$ to $\Omega_p t = 153.6$; and D, from $\Omega_p t = 204.8$ to $\Omega_p t = 256.0$, respectively.

AMPTE/CCE [*Anderson et al.*, 1994] and Wind [*Farrugia et al.*, 2004] spacecraft in the PDL. The two bands in the spectrum correspond to the proton cyclotron waves and helium cyclotron waves, and they are excited by the H^+ and He^{2+} temperature anisotropies respectively as proposed by *Denton et al.* [1993, 1994a]. This conclusion can be demonstrated more clearly in Figures 3a and 3b, which show the spectrum of the excited waves during four different time periods: A, from $\Omega_p t = 0$ to $\Omega_p t = 51.2$; B, from $\Omega_p t = 51.2$ to $\Omega_p t = 102.4$; C, from $\Omega_p t = 102.4$ to $\Omega_p t = 153.6$; and D, from $\Omega_p t = 204.8$ to $\Omega_p t = 256.0$ for run 2 and run 3, respectively. In run 2 we only consider the H^+ temperature anisotropy ($T_{\perp\alpha}/T_{\|\alpha} = 1$), and in run 3 only the He^{2+} temperature anisotropy ($T_{\perp p}/T_{\|p} = 1$). The main power in the spectrum for run 2 is above the helium gyrofrequency while the main power for run 3 is below the helium cyclotron waves. Their peaks in the spectrum are around $0.62\Omega_p$ and $0.25\Omega_p$, respectively. We can easily find that the two frequency bands shown in Figure 2 are excited by the H^+ and He^{2+} temperature anisotropies, respectively. From Figures 2 and 3, we also can find the following results: the dominant frequency of the proton cyclotron waves remains an almost constant, and the amplitude decreases in the nonlinear stage. In period C of Figure 2, the helium cyclotron waves are excited while the proton cyclotron waves still exist, therefore there are two frequency bands in the spectrum. In period D of Figure 2, the frequency band corresponding to the proton cyclotron waves disappears, and only the band corresponding to the helium cyclotron waves remains. The main power in the spectrum is below the helium gyrofrequency, which is similar the LOW category observed in the PDL [*Anderson et al.*, 1994].

[11] In general, the dominant frequency of the waves excited by temperature anisotropy decreases in the nonlinear stage like the helium cyclotron waves shown in Figures 2 and 3b ($T_{\perp p}/T_{\|p} = 1$). However, in Figures 2 and 3a ($T_{\perp\alpha}/T_{\|\alpha} = 1$) it is shown that the dominant frequency of the proton cyclotron waves remains as a

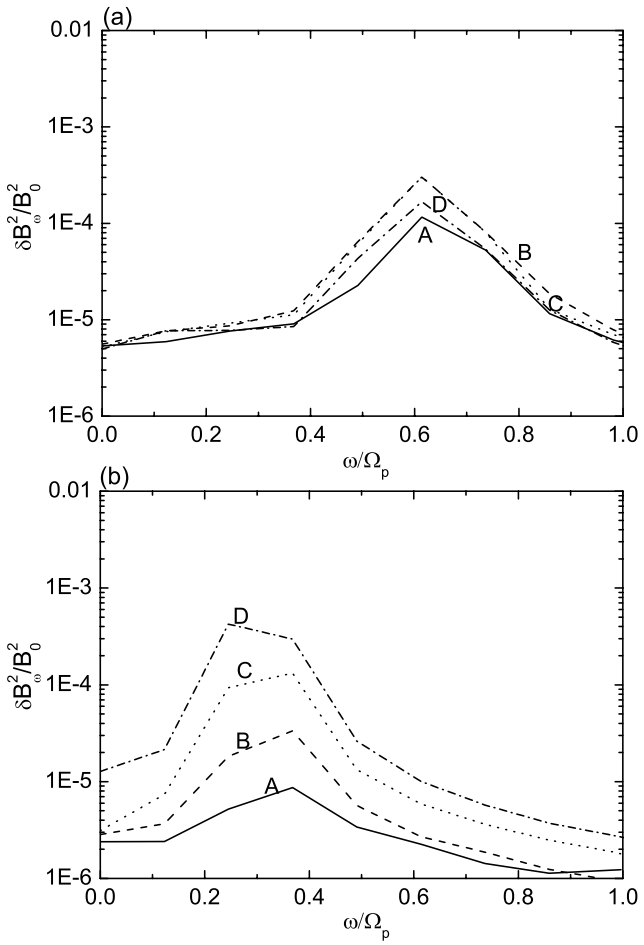

Figure 3. Frequency spectrum of the excited ion cyclotron waves during four different time periods for (a) run 2 and (b) run 3. The solid, dashed, dotted and dash-dotted lines represent periods A, from $\Omega_p t = 0$ to $\Omega_p t = 51.2$; B, from $\Omega_p t = 51.2$ to $\Omega_p t = 102.4$; C, from $\Omega_p t = 102.4$ to $\Omega_p t = 153.6$; and D, from $\Omega_p t = 204.8$ to $\Omega_p t = 256.0$, respectively.

constant. The reasons can be explained as follows: actually the dominant frequency of the proton cyclotron waves decreases in the nonlinear stage. However, when their frequencies decrease to around $0.5\Omega_p$, the proton cyclotron waves are resonantly absorbed by He^{2+}. Therefore it seems that its dominant frequency is kept as constant. This can be confirmed in Figure 4, which shows the spectrum of the excited waves during four different time periods: A, from $\Omega_p t = 0$ to $\Omega_p t = 51.2$; B, from $\Omega_p t = 51.2$ to $\Omega_p t = 102.4$; C, from $\Omega_p t = 102.4$ to $\Omega_p t = 153.6$; and D, from $\Omega_p t = 204.8$ to $\Omega_p t = 256.0$ for run 4, which neglect the effect of the He^{2+} ($\eta = 0$). In this run, only the proton cyclotron waves are excited. The dominant frequency decreases from about $0.62\Omega_p$ during period A to about $0.5\Omega_p$ during period D, and the amplitude is almost same. Therefore we can find that because of the resonant absorption of He^{2+} the dominant frequency of the proton cyclotron waves shown in Figures 2 and 3a is kept as a constant in the nonlinear stage.

[12] Figure 5a presents the time evolution of the H^+ and He^{2+} temperature anisotropies, and Figure 5b presents the spectrum of the excited waves during four different time periods for run 5, for which $\beta_{\|p} = 0.3$. Similar to run 1, the H^+ temperature anisotropy first decreases, and then the He^{2+} temperature anisotropy. At the quasi-equilibrium stage, the H^+ and He^{2+} temperature anisotropies are about 1.5 and 1.7, respectively. In run 5, with the increase of both the thermal velocity of He^{2+} and amplitude of the proton cyclotron waves excited by the H^+ temperature anisotropy, the He^{2+} resonant absorption around $0.5\Omega_p$ is overcome by the proton cyclotron waves. The increase of the thermal velocity can also broaden the spectrum of the excited waves. During period A, the proton cyclotron waves dominate the spectrum, and the helium cyclotron waves are negligible. The dominant frequency of the waves is larger than the helium gyrofrequency. In the nonlinear stage of the proton cyclotron waves, their frequencies decrease. During period B, the helium cyclotron waves are excited with the dominant frequency below the helium gyrofrequency, and their frequency band merges with that of the proton cyclotron waves. The spectrum during this period is continuous and the main power extends from ~ 0.1 up to $\sim 0.7\Omega_p$, which can explain the CON spectral category observed in the PDL. During periods C and D, the frequencies of the excited waves continue decreasing and form a spectrum with main power below the helium gyrofrequency, which can explain the LOW category observed in PDL. The spectrum of the excited waves during four different time periods: A, from $\Omega_p t = 0$ to $\Omega_p t = 51.2$; B, from $\Omega_p t = 51.2$ to $\Omega_p t = 102.4$; C, from $\Omega_p t = 102.4$ to $\Omega_p t = 153.6$; and D, from $\Omega_p t = 204.8$ to $\Omega_p t = 256.0$, for runs 6 and 7 is shown in Figure 6. Runs 6 and 7 consider the only effect of the H^+ and He^{2+} temperature anisotropy ($T_{\perp\alpha}/T_{\|\alpha} = 1$ and $T_{\perp p}/T_{\|p} = 1$, respectively), and they excite only the proton cyclotron waves and helium cyclotron waves, respectively. The frequencies of the proton cyclotron waves in run 6 decrease in their corresponding nonlinear stage. The saturation amplitude of the proton cyclotron waves is larger than that of run 2, and it is consistent with prediction that the saturation amplitude will increase with $\beta_{\|p}$ [*Gary and Winske*, 1993]. The spectrum

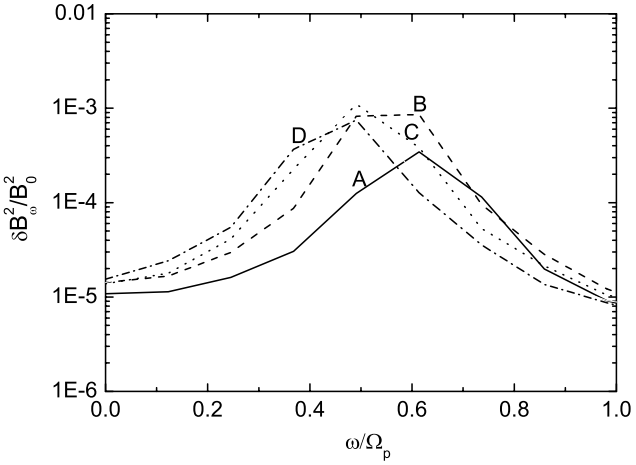

Figure 4. Frequency spectrum of the excited ion cyclotron waves during four different time periods for run 4. The solid, dashed, dotted and dash-dotted lines represent periods A, from $\Omega_p t = 0$ to $\Omega_p t = 51.2$; B, from $\Omega_p t = 51.2$ to $\Omega_p t = 102.4$; C, from $\Omega_p t = 102.4$ to $\Omega_p t = 153.6$; and D, from $\Omega_p t = 204.8$ to $\Omega_p t = 256.0$, respectively.

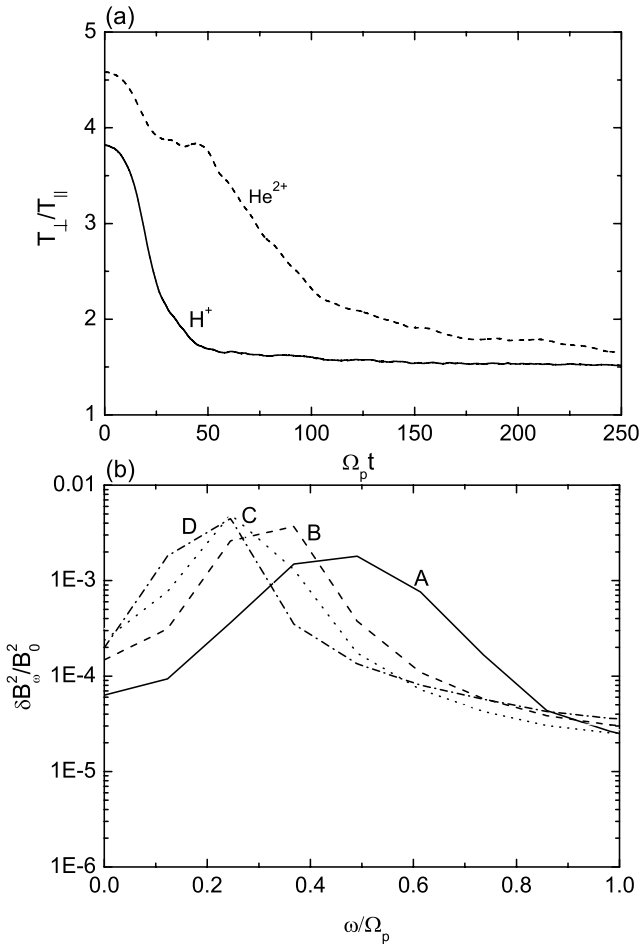

Figure 5. (a) Time evolution of the H^+ and He^{2+} temperature anisotropies for run 5; the solid and dashed lines represent the H^+ and He^{2+} temperature anisotropies, respectively. (b) Frequency spectrum of the excited waves during four different time periods for run 5, The solid, dashed, dotted and dash-dotted lines represent periods A, from $\Omega_p t = 0$ to $\Omega_p t = 51.2$; B, from $\Omega_p t = 51.2$ to $\Omega_p t = 102.4$; C, from $\Omega_p t = 102.4$ to $\Omega_p t = 153.6$; and D, from $\Omega_p t = 204.8$ to $\Omega_p t = 256.0$, respectively.

for run 5 is the result of the interactions between the proton cyclotron waves and helium cyclotron waves.

4. Discussion and Conclusions

[13] The frequency spectrum of the ion cyclotron waves observed in the PDL can be classified into three categories: LOW, CON and BIF [see *Anderson et al.*, 1994, Figure 1]. In this paper, we perform 1-D hybrid simulations to investigate the spectrum evolution of the ion cyclotron waves excited by the H^+ and He^{2+} temperature anisotropies in a homogeneous, magnetized plasma. How the linear polarization of the lower-frequency band is formed isn't discussed here, and it has been discussed by *Denton et al.* [1993]. The results show that the H^+ and He^{2+} temperature anisotropies excite the proton cyclotron waves and helium cyclotron waves, respectively. In their linear growth stage, the dominant frequency of the proton cyclotron waves is larger than the helium gyrofrequency $0.5\Omega_p$, while the dominant frequency of the helium cyclotron waves is smaller than the helium gyrofrequency. The proton cyclotron waves are first excited, and then the helium cyclotron waves. When $\beta_{\|p}$ is small, the dominant frequency of the proton cyclotron waves can be considered as a constant. The BIF category is formed in the spectrum after the helium cyclotron waves are excited. The two peaks of the BIF category are around $0.25\Omega_p$ and $0.62\Omega_p$, which correspond to the dominant frequencies of the helium cyclotron waves and proton cyclotron waves. When $\beta_{\|p}$ is large, the spectrum of waves become broad. The dominant frequency of the proton cyclotron waves decreases in the nonlinear stage, and their frequency band merges with that of the helium cyclotron waves after the helium cyclotron waves are excited. This can explain the CON category observed in the PDL. The LOW category is formed at the quasi-equilibrium stage after the proton cyclotron waves are resonantly absorbed by He^{2+} for small $\beta_{\|p}$ or after their frequencies are drifted to smaller than the helium gyrofrequency for large $\beta_{\|p}$. Another possibility for the formation of the LOW category is that the initial temperature anisotropies are sufficiently small,

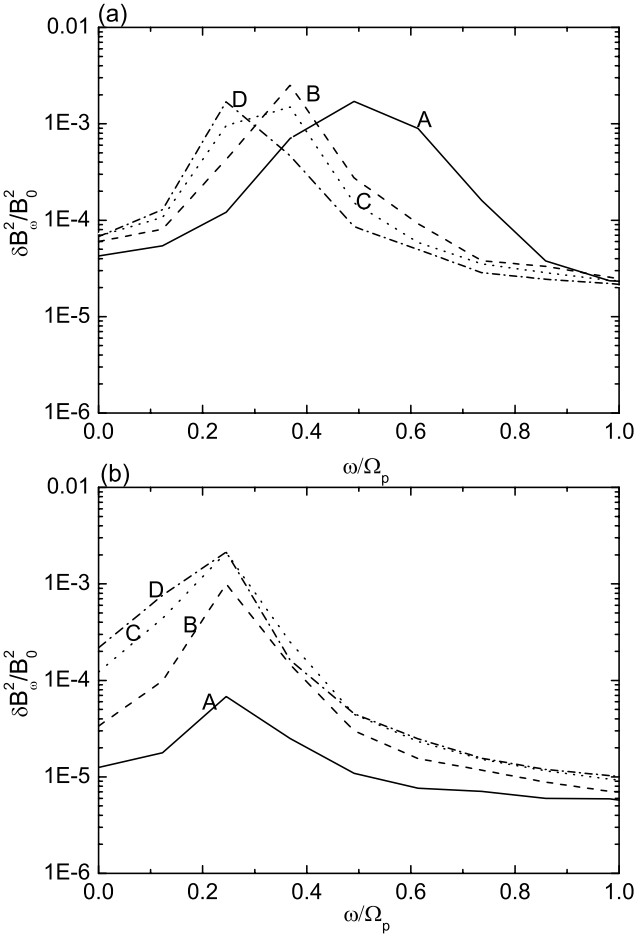

Figure 6. Frequency spectrum of the excited ion cyclotron waves during four different time periods for (a) run 6 ($T_{\perp\alpha}/T_{\|\alpha} = 1$) and (b) run 7 ($T_{\perp p}/T_{\|p} = 1$). The solid, dashed, dotted and dash-dotted lines represent periods A, from $\Omega_p t = 0$ to $\Omega_p t = 51.2$; B, from $\Omega_p t = 51.2$ to $\Omega_p t = 102.4$; C, from $\Omega_p t = 102.4$ to $\Omega_p t = 153.6$; and D, from $\Omega_p t = 204.8$ to $\Omega_p t = 256.0$, respectively.

which has been discussed by *Denton et al.* [1994a]. In such a situation, because for both the proton cyclotron waves and helium cyclotron waves their frequencies are less than $A/(A+1)$ (where $A = T_\perp/T_\parallel - 1$), the frequencies of the excited ion cyclotron waves will be smaller than $0.5\Omega_p$.

[14] In summary, the BIF category of the ion cyclotron waves in the PDL is formed when $\beta_{\|p}$ is small, while the CON category is generated when $\beta_{\|p}$ is large. This is consistent with the results of the spacecraft observations [*Anderson et al.*, 1994] and linear Vlasov theory [*Denton et al.*, 1993, 1994a; *Gnavi et al.*, 2000]: the CON category tends to occur where $\beta_{\|p}$ is larger than the BIF category. The CON and BIF categories are formed just after the helium cyclotron waves are excited, and at that time the frequency decrease of the ion cyclotron waves doesn't have obvious effect on the spectrum. The LOW category is the results of the nonlinear evolution of the ion cyclotron waves.

[15] **Acknowledgments.** This research was supported by the National Science Foundation of China (NSFC) under grants 40304012 and 40336052.

[16] Lou-Chuang Lee thanks Richard Denton and Peter Gary for their assistance in evaluating this paper.

References

Anderson, B. J. (1995), ULF signals observed near the magnetopause, in *Physics of the Magnetopause, Geophys. Monogr. Ser.*, vol. 90, edited by P. Song, B. U. Sonnerup, and M. F. Thomsen, p. 269, AGU, Washington, D. C.

Anderson, B. J., and S. A. Fuselier (1993), Magnetic pulsations from 0.1 to 4.0 Hz and associated plasma properties in the Earth's subsolar depletion magnetosheath and plasma depletion layer, *J. Geophys. Res.*, *98*, 1461–1479.

Anderson, B. J., S. A. Fuselier, and D. Murr (1991), Electromagnetic ion cyclotron waves observed in the plasma depletion layer, *Geophys. Res.Lett.*, *18*, 1955–1958.

Anderson, B. J., S. A. Fuserlier, S. P. Gary, and R. E. Denton (1994), Magnetic spectral signatures in the Earth's magnetosheath and plasma depletion layer, *J. Geophys. Res.*, *99*, 5877–5891.

Crooker, N. U., T. E. Eastman, and G. S. Stiles (1979), Observations of plasma depletion in the magnetosheath at the dayside magnetopause, *J. Geophys. Res.*, *84*, 869–882.

Denton, R. E., and J. G. Lyon (2000), Effect of pressure anisotropy on the structure of a two-dimensional magnetosheath, *J. Geophys. Res.*, *105*, 7545–7556.

Denton, R. E., M. K. Hudson, S. A. Fuselier, and B. J. Anderson (1993), Electromagnetic ion cyclotron waves in the plasma depletion layer, *J. Geophys. Res.*, *98*, 13,477–13,490.

Denton, R. E., S. P. Gary, B. J. Anderson, S. A. Fuselier, and M. K. Hudson (1994a), Low-frequency magnetic fluctuation spectra in the magnetosheath and plasma depletion layer, *J. Geophys. Res.*, *99*, 5893–5901.

Denton, R. E., B. J. Anderson, S. P. Gary, and S. A. Fuselier (1994b), Bounded anisotropy fluid model for ion temperatures, *J. Geophys. Res.*, *99*, 11,225–11,242.

Denton, R. E., S. P. Gary, X. Li, B. J. Anderson, J. W. LaBelle, and M. Lessard (1995), Low-frequency fluctuations in the magnetosheath near the magnetopause, *J. Geophys. Res.*, *100*, 5665–5679.

Erkaev, N. V., C. J. Farrugia, and H. K. Biernat (1999), Three-dimensional, one-fluid, ideal MHD model of magnetosheath flow with anisotropic pressure, *J. Geophys. Res.*, *104*, 6877–6887.

Erkaev, N. V., H. K. Biernat, and C. J. Farrugia (2000), Ideal magnetohydrodynamic flow around a blunt body under anisotropic pressure, *Phys. Plasmas*, *7*, 3413–3420.

Farrugia, C. J., G. Gnavi, F. T. Gratton, H. Matsui, R. B. Torbert, R. P. Lepping, M. Oieroset, and R. P. Lin (2004), Electromagnetic ion cyclotron waves in the subsolar region under normal dynamic pressure: Wind observations and theory, *J. Geophys. Res.*, *109*, A02202, doi:10.1029/2003JA010104.

Fuselier, S. A., and W. K. H. Schmidt (1997), Solar wind He^{2+} ring-beam distributions downstream from the Earth's bow shock, *J. Geophys. Res.*, *102*, 11,273–11,280.

Fuselier, S. A., B. J. Anderson, S. P. Gary, and R. E. Denton (1994), Inverse correlations between the ion temperature anisotropy and the plasma beta in the Earth's quasi-parallel magnetosheath, *J. Geophys. Res.*, *99*, 14,931–14,936.

Gary, S. P. (1992), The mirror and ion cyclotron anisotropy instabilities, *J. Geophys. Res.*, *97*, 8519–8529.

Gary, S. P., and D. Winske (1993), Simulations of ion cyclotron anisotropy instabilities in the terrestrial magnetosheath, *J. Geophys. Res.*, *98*, 9171–9179.

Gary, S. P., S. A. Fuselier, and B. J. Anderson (1993a), Ion anisotropy instabilities in the magnetosheath, *J. Geophys. Res.*, *98*, 1481–1488.

Gary, S. P., M. E. McKean, and D. Winske (1993b), Ion cyclotron anisotropy instabilities in the magnetosheath: Theory and simulations, *J. Geophys. Res.*, *98*, 3963–3972.

Gary, S. P., M. E. McKean, D. Winske, B. J. Anderson, R. E. Denton, and S. A. Fuselier (1994a), The proton cyclotron instability and the anisotropy/beta inverse correlation, *J. Geophys. Res.*, *99*, 5903–5914.

Gary, S. P., P. D. Convery, R. E. Denton, S. A. Fuselier, and B. J. Anderson (1994b), Proton and helium cyclotron anisotropy instability thresholds in the magnetosheath, *J. Geophys. Res.*, *99*, 5915–5921.

Gary, S. P., J. Wang, D. Winske, and S. A. Fuselier (1997), Proton temperature anisotropy upper bound, *J. Geophys. Res.*, *102*, 27,159–27,169.

Gnavi, G., F. T. Gratton, and C. J. Farrugia (2000), Theoretical properties of electromagnetic ion cyclotron waves in the terrestrial, dayside, low-latitude plasma depletion layer under uncompressed magnetosheath conditions, *J. Geophys. Res.*, *105*, 20,973–20,987.

Gratton, F. T., and C. J. Farrugia (1996), Electromagnetic ion cyclotron waves in the terrestrial plasma depletion layer: Effects of possible differential speeds between H^+ and He^{2+} ions, *J. Geophys. Res.*, *101*, 21,553–21,560.

Hellinger, P., and P. Travnicek (2005), Magnetosheath compression: Role of characteristic compression time, alpha particle abundance, and alpha/proton relative velocity, *J. Geophys. Res.*, *110*, A04210, doi:10.1029/2004JA010687.

Leory, M., D. Winske, C. C. Goodrich, C. S. Wu, and K. Papadoulos (1982), The structure of perpendicular bow shock, *J. Geophys. Res.*, *87*, 5081–5094.

Lu, Q. M., and S. Wang (2005), Formation of He^{2+} shell-like distributions downstream of the Earth's bow shock, *Geophys. Res. Lett.*, *32*, L03111, doi:10.1029/2004GL021508.

McKean, M. E., D. Winske, and S. P. Gary (1992), Mirror and ion cyclotron anisotropy instabilities in the magnetosheath, *J. Geophys. Res.*, *97*, 19,421–19,432.

McKean, M. E., N. Omidi, and D. Krauss-Varban (1995), Wave and ion evolution downstream of quasi-perpendicular bow shocks, *J. Geophys. Res.*, *100*, 3427–3437.

Midgley, J. E., and L. Davis (1963), Calculation by a moment technique of the perturbation of the geomagnetic field by the solar wind, *J. Geophys. Res.*, *68*, 5111–5123.

Paschmann, G., N. Sckopke, G. Haerendel, I. Papamastorakis, S. J. Bame, J. R. Asbridge, J. T. Gosling, E. W. Homes Jr., and E. R. Tech (1978), ISEE plasma observations near the subsolar magnetopause, *Space Sci. Rev.*, *22*, 717–737.

Phan, T. D., G. Paschmann, W. Baumjohann, N. Sckopke, and H. Luhr (1994), The magnetosheath region adjacent to the dayside magnetopause: AMPTE/IRM observations, *J. Geophys. Res.*, *99*, 121–141.

Pudovkin, M. I., B. P. Besser, V. V. Lebedeva, S. A. Zaitseva, and C. V. Meister (1999), Magnetosheath model in the Chew-Goldberger-Low approximation, *Phys. Plasmas*, *6*, 2887–2896.

Samsonov, A. A., M. I. Pudovkin, S. P. Gary, and D. Hubert (2001), Anisotropic MHD model of the dayside magnetosheath downstream of the oblique bow shock, *J. Geophys. Res.*, *106*, 21,689–21,699.

Sckopke, N., G.. Paschmann, A. L. Brinca, C. W. Carlson, and H. Luhr (1990), Ion thermalization in quasi-perpendicular shocks involving reflected ions, *J. Geophys. Res.*, *95*, 6337–6352.

Winske, D. (1985), Hybrid simulation codes with application to shocks and upstream waves, *Space Sci. Rev.*, *42*, 53–66.

Winske, D., and K. B. Quest (1988), Magnetic field and density fluctuations at perpendicular supercritical collisionless shocks, *J.Geophys. Res.*, *93*, 9681–9693.

Wu, C. C. (1992), MHD flow past an obstacle: Large-scale flow in the magnetosheath, *Geophys. Res. Lett.*, *19*, 87–90.

Zwan, B. J., and R. A. Wolf (1976), Depletion of solar wind plasma near a planetary boundary, *J. Geophys. Res.*, *81*, 1636–1648.

F. Guo, Q. M. Lu, and S. Wang, CAS Key Laboratory of Basic Plasma Physics, School of Earth and Space Sciences, University of Science and Technology of China, Hefei, Anhui 230026, China. (qmlu@ustc.edu.cn)